AGU PUBLICATIONS

Water Resources Research

RESEARCH ARTICLE

10.1002/2017WR022116

Key Points:
- The subsurface is viewed as a natural mixer due to the spatiotemporal variability of the flow field
- Systematic analysis of the interplay between parameters controlling the spatial and temporal variability of the flow field on dilution
- New analytical first-order solution to predict dilution enhancement in transient and spatially heterogeneous 3-D subsurface flows

Correspondence to:
M. Di Dato,
mariaines.didato@unitn.it

Citation:
Di Dato, M., de Barros, F. P. J., Fiori, A., & Bellin, A. (2018). Improving the efficiency of 3-D hydrogeological mixers: Dilution enhancement via coupled engineering-induced transient flows and spatial heterogeneity. *Water Resources Research*, *54*. https://doi.org/10.1002/2017WR022116

Received 23 OCT 2017
Accepted 1 MAR 2018
Accepted article online 6 MAR 2018

Improving the Efficiency of 3-D Hydrogeological Mixers: Dilution Enhancement Via Coupled Engineering-Induced Transient Flows and Spatial Heterogeneity

Mariaines Di Dato[1], Felipe P. J. de Barros[2], Aldo Fiori[3], and Alberto Bellin[1]

[1]Department of Civil, Environmental and Mechanical Engineering, University of Trento, Trento, Italy, [2]Sonny Astani Department of Civil and Environmental Engineering, University of Southern California, Los Angeles, CA, USA, [3]Dipartimento di Ingegneria, Roma Tre University, Rome, Italy

Abstract Natural attenuation and in situ oxidation are commonly considered as low-cost alternatives to ex situ remediation. The efficiency of such remediation techniques is hindered by difficulties in obtaining good dilution and mixing of the contaminant, in particular if the plume deformation is physically constrained by an array of wells, which serves as a containment system. In that case, dilution may be enhanced by inducing an engineered sequence of injections and extractions from such pumping system, which also works as a hydraulic barrier. This way, the aquifer acts as a natural mixer, in a manner similar to the industrialized engineered mixers. Improving the efficiency of hydrogeological mixers is a challenging task, owing to the need to use a 3-D setup while relieving the computational burden. Analytical solutions, though approximated, are a suitable and efficient tool to seek the optimum solution among all possible flow configurations. Here we develop a novel physically based model to demonstrate how the combined spatiotemporal fluctuations of the water fluxes control solute trajectories and residence time distributions and therefore, the effectiveness of contaminant plume dilution and mixing. Our results show how external forcing configurations are capable of inducing distinct time-varying groundwater flow patterns which will yield different solute dilution rates.

1. Introduction

One of the most challenging issues in subsurface hydrology and environmental engineering is the development of efficient and cost-effective techniques for remediating contaminated aquifers, while containing the propagation of the contamination during the clean-up activities. In general, contaminant site management aims to achieve two objectives: the first one is the prevention of contaminant release from an ongoing source, while the second objective consists on the treatment of the polluted aquifer. The latter goal is achieved by removing or, at least, reducing the concentration levels of toxic chemicals of concern (see Freeze & Cherry, 1979, chapter 9). The reduction of pollutant concentration to regulatory standards is typically difficult to achieve from both technical and economical perspectives (Bredehoeft, 1992). Pump and treat is by far the most used technique for aquifer remediation (Mackay & Cherry, 1989) despite its high costs of operation in order to comply with regulatory standards (de Barros et al., 2013; Haley et al., 1991; National Research Council, 1994; Zhang & Brusseau, 1999). Inefficiency of pump and treat methods can be attributed to trapped contaminants in low-conductive zones. The contaminant mass trapped in these low-conductivity layers is difficult to mobilize by the action of pumping (e.g., de Barros et al., 2013; LaBolle & Fogg, 2001). Possible alternatives to pump and treat are in situ oxidation and natural attenuation, which may be preferred due to lower financial costs, although the remediation time may be larger (Mulligan et al., 2001). To be effective, in situ remediation requires that the contaminant mixes with clean groundwater or treatment solution. This is the most complex problem one faces when adopting remediation strategy in situ, given that at the operational (field) scale mixing is impeded by the low pore-velocity with heterogeneity exerting a counteracting effect (i.e., it enhances mixing) by increasing local concentration gradients associated with plume's deformation (e.g., Boso & Bellin, 2012).

It is widely accepted that the spatial variability of subsurface hydrogeological properties leads to fluctuations in the velocity field, which enhances solute mixing through the rich interplay between advection and

diffusion (e.g., Boso & Bellin, 2012; Cirpka et al., 2012; de Barros et al., 2012, 2015; Dentz & de Barros, 2015; Fiori & Dagan, 2000; Kapoor & Kitanidis, 1998; Weeks & Sposito, 1998). Aside from the natural spatial heterogeneity of the subsurface, one may attempt to modify externally, through the action of pumping, the flow field configuration such as to magnify the dilution effect. This can be attained by making use of a system (or battery) of pumping wells (Environmental Protection Agency, 1998; Kitanidis & McCarty, 2012; Luo et al., 2006; Suthersan et al., 2015). Unsteady flow field, produced by oscillatory pumping wells, has been proposed in hydraulic tomography for inferring the aquifer properties (e.g., Cardiff & Barrash, 2015; Cardiff et al., 2013; Dagan & Rabinovich, 2014; Johnson et al., 1966; Kuo, 1972; Rabinovich et al., 2015; Renner & Messar, 2006). To the best of our knowledge, only a limited number of works consider the impact of transient flow fluctuations on transport in spatially heterogeneous aquifers (e.g., Chang et al., 1992; Cirpka & Attinger, 2003; Dentz & Carrera, 2005; Libera et al., 2017; Neupauer et al., 2014). Recently, Libera et al. (2017) showed how transient well pumping operations may attenuate the concentration breakthrough curve in a water supply zone and discussed how the combined effect of natural heterogeneity and engineering factors (i.e., pumping operations) controls the risk of exposure at a contaminated site. Similar to industrialized engineered mixers (e.g., Ottino, 1989), the aforementioned works strengthen the idea that the subsurface formation can be viewed as a *natural mixer*. Such a system should be properly geoengineered with the goal of taking full advantage of shear flow features induced by the heterogeneous structure of the permeability field. As shown in de Barros et al. (2012), localized shear flows have a significant impact on augmenting dilution (see also Benekos et al., 2006).

With the purpose of developing efficient techniques to improve water quality in polluted aquifers, several works (e.g., Bagtzoglou & Oates, 2007; Metcalfe et al., 2010; Trefry et al., 2012; Zhang et al., 2009) have designed models of groundwater remediation based on the theory of chaotic advection (e.g., Jones & Aref, 1988; Ottino, 1989; Sposito, 2006; Trefry et al., 2012). Along this line of work, Mays and Neupauer (2012) have developed a novel framework to enhance solute dilution denoted as *Engineered Injection and Extraction*. This technique consists of an array of wells operating in a designed manner to achieve an unsteady flow, which forces the plume to be transported within a constrained region (which is important for regulatory purposes). As a consequence of the constrained trajectory induced by the wells, the plume experiences a limited amount of heterogeneity and proper engineered well operation can be adopted to augment the mixing effect.

The work of Mays and Neupauer (2012) investigates how an engineered sequence of extraction and injection enhances stretching and folding under pure advective transport. Successively, Piscopo et al. (2013) and Neupauer et al. (2014) have refined the model of Mays and Neupauer (2012) by considering advection, dispersion, and reaction. Neupauer et al. (2014) systematically quantified the efficiency of remediation as a function of the coupled effect of aquifer heterogeneity and engineering-induced velocity oscillations. The injection-extraction scheme proposed by Mays and Neupauer (2012), and used in the subsequent studies (e.g., Neupauer et al., 2014; Piscopo et al., 2013, 2015), can be cast within an optimization framework (Piscopo et al., 2015, 2016). A system of engineering alternate pumping was applied also by Rodríguez-Escales et al. (2017) to develop a reactive transport model for improving degradation of organic compound. However, the analysis carried out by the above mentioned studies (e.g., Neupauer et al., 2014; Piscopo et al., 2013, 2015; Rodríguez-Escales et al., 2017) is based on numerical solutions with a given flow configuration and limited to 2-D domains. The additional degree of freedom of 3-D systems may further attenuate the concentration field. In addition, a number of operational parameters should be decided, from wells configuration to pumping sequence. Investigating numerically how these parameters interact and the corresponding influence on the mixer's effectiveness is difficult and computationally costly.

Motivated by the pioneering works of Piscopo et al. (2013, 2015) and Neupauer et al. (2014), our work aims to develop a novel semianalytical solution for solute mixing in a 3-D spatially heterogeneous aquifer, while accounting for the transients in the flow field induced by the presence of an engineered injection-extraction system. Our solution is based on the concept of Lagrangian concentration, introduced by Fiori (2001). The Lagrangian concentration framework was verified against field experiments and numerical simulations (Boso et al., 2013; de Barros et al., 2015) and applied to quantify the risks of adverse health effects (de Barros & Fiori, 2014; Zarlenga et al., 2016). In this paper, we adopt the Lagrangian concentration framework to evaluate solute dilution in a typical remediation context similar to that used by Neupauer et al. (2014). The solute mixing efficiency is quantified by means of the dilution index (Kitanidis, 1994). We

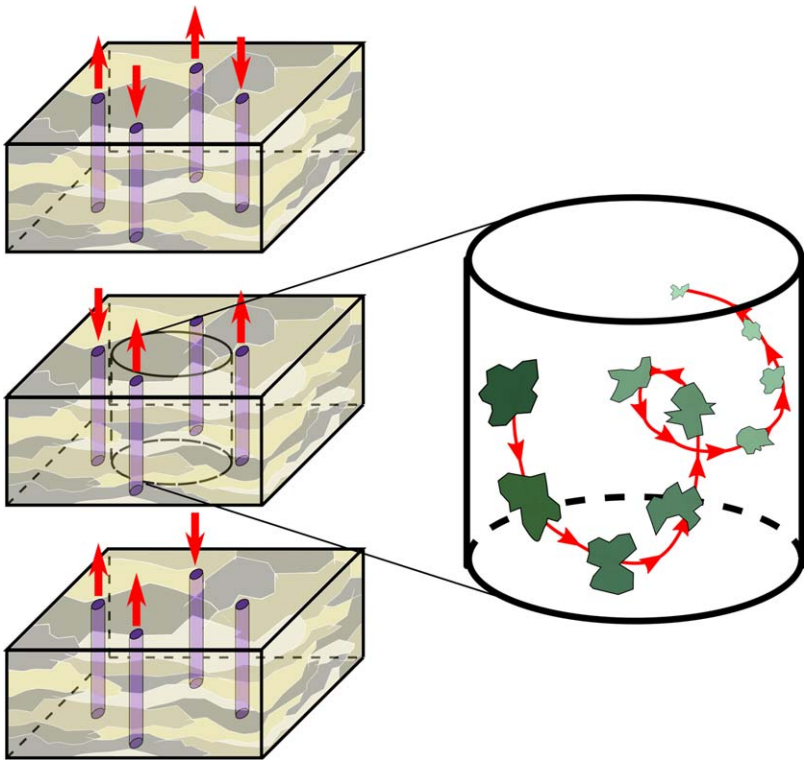

Figure 1. A sketch of the conceptual model for a 3-D heterogeneous aquifer with spatiotemporal fluctuations of the the flow field. The geological formation can be viewed as a *natural mixer*. Spatial variability stems from the natural heterogeneity of the hydrogeological properties of the medium. Temporal fluctuations of the flow can be attributed to engineered factors induced by alternate pumping.

investigate how closed flow paths, forced by different injection-extraction pumping sequences, lead to different dilution rates. Due to the analytical features, the model is computationally efficient and allows to evaluate the sensitivity of remediation to key geostatistical parameters. Furthermore, the semianalytical solution enables to capture the rich interplay between aquifer heterogeneity, local-scale dispersion and fluctuations in the mean flow in controlling dilution. A sketch depicting the general conceptual model adopted for the 3-D field scale mixer is illustrated in Figure 1. The combined effect of the temporal fluctuations in the flow field (e.g., due to external factors such as injection and extraction rates) with natural heterogeneity modifies the plume's trajectory and therefore its residence times and deformation rates. The paper is organized as follows: the general mathematical framework together with the governing equations is presented in sections 2 and 3, respectively; in section 4, we discuss the sensitivity of the dilution index toward different parameters; the method is then applied to the Cape Cod site in section 5. The main findings are summarized in the last section.

2. Problem Statement

Our main objective is to analytically quantify the effectiveness of enforced transient flow configurations in enhancing dilution of a solute plume within the flow domain $\mathcal{W}$. Engineering parameters (i.e., injection and extraction rates) are included into the vector Θ_E, while hydrogeological parameters, which define the properties of the aquifer (i.e., porosity, hydraulic conductivity, and geostatistical variables) are incorporated into the vector Θ_N.

We start by considering an incompressible flow in a 3-D porous formation with constant porosity n and spatially heterogeneous, locally isotropic, log-conductivity field $Y(\boldsymbol{x})=\ln K(\boldsymbol{x})$, where $\boldsymbol{x}=(x_1, x_2, x_3)$ is the Cartesian coordinate system. As customary, $Y(\boldsymbol{x})$ is modeled as a normally distributed Random Space Function (RSF) characterized by the mean $\langle Y\rangle$ and the variance σ_Y^2, both considered to be constant. In this work, the angled brackets $\langle\cdot\rangle$ indicate the ensemble mean operator. The correlation structure is defined by the

covariance function $C_Y(\boldsymbol{r})=\langle Y'(\boldsymbol{x})Y'(\boldsymbol{y})\rangle$, where $Y'=Y-\langle Y\rangle$ is the fluctuation around the mean and $\boldsymbol{r}=\boldsymbol{x}-\boldsymbol{y}$ indicates the lag distance between $\boldsymbol{x}$ and $\boldsymbol{y}$. The integral scales are I and I_V in the horizontal and vertical directions, respectively. Based on the data summarized in Rubin (2003, Table 2.2), we consider a statistically anisotropic formation (i.e., $I \neq I_V$).

A plume of contaminant is instantaneously released into the aquifer. Here the solute undergoes advection and dispersion at local-scale and macroscale. The spatiotemporal evolution of the concentration field c is governed by the advection-dispersion equation:

$$\frac{\partial c(\mathbf{x},t|\Theta_N,\Theta_E)}{\partial t}+\mathbf{V}(\mathbf{x},t|\Theta_N,\Theta_E)\cdot\nabla c(\mathbf{x},t|\Theta_N,\Theta_E)-\nabla\cdot[\mathbf{D}\nabla c(\mathbf{x},t|\Theta_N,\Theta_E)]=0, \tag{1}$$

where $\mathbf{V}$ is the spatially variable Darcy-scale velocity field and $\mathbf{D}$ is the local-dispersion tensor. The spatial variability of the velocity field stems from the heterogeneity in the hydrogeological properties of the aquifer (e.g., hydraulic conductivity), while its temporal fluctuations are an outcome of the flow transients, which are induced by a system of alternate pumping such as the one depicted in Figure 1.

Under the hypothesis that larger dilution implies an effective remediation, as shown for example by Rodríguez-Escales et al. (2017), we consider here the dilution index E, introduced by Kitanidis (1994), as a global metric describing the efficiency of the natural hydrogeological mixer. An extensive review of other mixing metrics is provided in the work by Dentz et al. (2011). The dilution index is defined as follows (Kitanidis, 1994):

$$E(t|\Theta_N,\Theta_E)=\exp[\mathcal{H}(t|\Theta_N,\Theta_E)], \tag{2}$$

where the entropy $\mathcal{H}$ is given by

$$\mathcal{H}(t|\Theta_N,\Theta_E)=-\int_{\mathcal{W}}\frac{c(\boldsymbol{x},t|\Theta_N,\Theta_E)}{M_0}\ln\left[\frac{c(\boldsymbol{x},t|\Theta_N,\Theta_E)}{M_0}\right]d\boldsymbol{x}, \tag{3}$$

with M_0 denoting the mass of contaminant. The entropy quantifies the disorder in the spatial distribution of the solute: similarly to classic thermodynamics, large levels of disorder imply higher $\mathcal{H}$ values.

As shown in Libera et al. (2017), the coupled action originating from the parameters present in both Θ_N and Θ_E has a significant impact in enhancing the attenuation of the solute concentration and the risks associated with groundwater contamination. The magnitude of E in equation (2) depends on both Θ_E and Θ_N, which characterize the engineered and natural systems, respectively. Our mathematical analysis aims to functionally relate equation (2) with the spatiotemporal patterns of the velocity field $\mathbf{V}$, which in turn depends on Θ_E and Θ_N. Details of the methodological steps utilized to solve flow and transport are given in the following section.

3. Modeling Approach

3.1. Overview

In this section, we describe the methodological steps and approximations needed to establish a functional relationship between E and the parameters Θ_E and Θ_N. Given the complexity of the problem, the following assumptions are considered in order to obtain an analytical solution for the dilution index:

1. The forced transient flow takes place in an unbounded domain, without sources or sinks.
2. Low-to-moderate heterogeneity in the Y-field, such that the *First-Order Approximation* (FOA) for the flow equation and E can be applied. This implies that the solution provided is formally valid for $\sigma_Y^2 \lesssim 1$ (see e.g., Bellin et al., 1992).
3. Quasi steady state conditions, such that the transient mean flow is modeled as a sequence of steady states over the unbounded flow domain $\mathcal{W}$. This assumption implies that the temporal scale of fluctuations induced by alternate pumping is much larger than $t_a=I^2S_{s,G}/K_G$, where K_G and $S_{s,G}$ are the geometric mean of the hydraulic conductivity and the storage coefficient, respectively.
4. Contaminant plumes originate from point-like sources (i.e., the characteristic dimension of the source zone is smaller than the integral scales of Y).

3.2. First-Order Approximation of the Flow Field

Under the assumption that changes in flow configuration (engineering-induced by pumping) are slow with respect to the characteristic time of the ensuing transient condition (item 3 in the list of section 3.1), the flow equation assumes the following form:

$$\nabla \cdot \left\{ \frac{K_G}{n} \exp\left[Y'(\boldsymbol{x}|\Theta_N)\right] \nabla H(\boldsymbol{x}, t|\Theta_N, \Theta_E) \right\} = 0, \tag{4}$$

where H is the fluctuating head, which is decomposed as $H = \langle H \rangle + h$, where $\langle H \rangle$ is the mean hydraulic head and h is the fluctuation. With this decomposition, equation (4) assumes the following form:

$$\nabla^2 \langle H \rangle + \nabla^2 h(\boldsymbol{x}, t|\Theta_N, \Theta_E) + \nabla Y'(\boldsymbol{x}|\Theta_N) \cdot \left[\nabla \langle H \rangle + \nabla h(\boldsymbol{x}, t|\Theta_N, \Theta_E)\right] = 0. \tag{5}$$

Ensemble averaging of equation (5) leads to the governing equation for the mean hydraulic head (see e.g., Dagan et al., 1996):

$$\nabla^2 \langle H \rangle = 0, \tag{6}$$

which leads to the following expression for the mean head: $\langle H \rangle = -\boldsymbol{J}(t|\Theta_E) \cdot \boldsymbol{x}$. Note that $\boldsymbol{J}$ is the spatially uniform and time-dependent mean head gradient. Such flow solution was applied in previous works (e.g., Bellin et al., 1996; Dagan et al., 1996; Farrell et al., 1994; Naff et al., 1988; Rehfeldt & Gelhar, 1992) to study how transport is affected by seasonal variations of the mean head gradient, with a good agreement with natural-gradient field tests (e.g., Freyberg, 1986). In the present work, the variation of mean head gradient is controlled by the engineering parameters, i.e., how many wells are operating and how often they switch between pumping and injection. The aforementioned studies shown that such a flow model is accurate if the scale characterizing the time variation of $\boldsymbol{J}$ is sufficiently large. Therefore, the validity of our solution is limited by the scheduled pumping operations.

Under these conditions, the velocity field $\boldsymbol{V} = -K(\boldsymbol{x}) \nabla H(t, \boldsymbol{x})/n$ can be decomposed into a temporally variable mean $\boldsymbol{U}(t|\Theta_E) \equiv \langle \boldsymbol{V} \rangle$, dependent on the engineering parameters, and a fluctuation $\boldsymbol{u}(\boldsymbol{x}, t|\Theta_N, \Theta_E)$ varying both in space and time. Following Dagan et al. (1996), the transient mean velocity $\boldsymbol{U}$ and fluctuation $\boldsymbol{u}$ can be approximated at first order as follows:

$$\begin{aligned} \boldsymbol{U}(t|\Theta_E) &= \frac{K_G}{n} \boldsymbol{J}(t|\Theta_E), \\ \boldsymbol{u}(\boldsymbol{x}, t|\Theta_N, \Theta_E) &= \frac{K_G}{n} \left[\boldsymbol{J}(t|\Theta_E) Y'(\boldsymbol{x}|\Theta_N) - \nabla h(\boldsymbol{x}, t|\Theta_N, \Theta_E)\right]. \end{aligned} \tag{7}$$

Notice that the fluctuation is a function of the coupled effect of medium heterogeneity and engineering-induced flow, while the mean depends only on the former.

In line with Dagan et al. (1996), the flow problem is solved in a rigorous mathematical framework based on the FOA in σ_Y^2, by which the equation for head fluctuation h is obtained by subtracting equation (6) from equation (5):

$$\nabla^2 h(\boldsymbol{x}, t|\Theta_N, \Theta_E) = \boldsymbol{J}(t|\Theta_E) \cdot \nabla Y'(\boldsymbol{x}|\Theta_N). \tag{8}$$

This approximation is accurate for low-to-moderate heterogeneous porous media up to $\sigma_Y^2 \lesssim 1$ (see assumption 2 in section 3.1; Bellin et al., 1992). The problem can be conveniently solved in the Fourier space, leading to the following expression for the Fourier transform of the velocity covariance (details on the derivation are provided in Appendix A):

$$\hat{u}_{ij}(\boldsymbol{k}, t', t''|\Theta_N, \Theta_E) = \sum_{p=1}^{3} \sum_{q=1}^{3} U_p(t'|\Theta_E)\, U_q(t''|\Theta_E) \left(\delta_{pi} - \frac{k_i k_p}{k^2}\right) \left(\delta_{qj} - \frac{k_j k_q}{k^2}\right) \hat{C}_Y(\boldsymbol{k}|\Theta_N), \tag{9}$$

where $\boldsymbol{k} = (k_1, k_2, k_3)$ is the wave number vector with $k = |\boldsymbol{k}|$ denoting its L-2 norm, δ_{ij} is the Kronecker's delta and $\hat{C}_Y$ is the Fourier transform of the log-conductivity covariance. Expressions for $\hat{C}_Y$ for different correlation models are provided in Rubin (2003, chapter 2). For the upcoming illustrations in section 4, we adopt a Gaussian axial-symmetric covariance model for Y:

$$C_Y(r_1, r_2, r_3) = \sigma_Y^2 \exp\left[-\frac{\pi}{4}\left(\frac{r_1^2 + r_2^2}{I^2} + \frac{r_3^2}{I_v^2}\right)\right], \tag{10}$$

where r_i corresponds to the lag distance between two points in the i-th direction, with $i = (1–3)$. The velocity covariance (9) requires the Fourier transform of equation (10), which reads

$$\hat{C}_Y(k_1.k_2,k_3)=\sqrt{\frac{8}{\pi^3}}\sigma_Y^2 el^3 \exp\left[-\frac{l^2(k_1+k_2+k_3)}{\pi}\right], \tag{11}$$

where $e = l/l_v$ is the statistical anisotropy ratio.

3.3. The Dilution Index for a Solute in a Lagrangian Framework

Equation (1) describes the spatiotemporal evolution of the solute concentration undergoing the coupled effect of natural factors (represented by the spatial variability of hydraulic conductivity and local-scale dispersion) and engineered-induced unsteady velocity field. The relative effect of advection and dispersion is quantified by the Peclet number $Pe = l/\alpha_d$, where the local-scale dispersivity α_d is assumed to be isotropic and constant.

In a recent paper, de Barros et al. (2015) determined an analytical solution for the dilution index (see equation (2)). The solution accounts for a spatially heterogeneous Y-field and steady state flow conditions. Their approach is here extended to transient flow under the hypothesis depicted in section 3.1.

Our derivation considers a solute with uniform concentration C_0 that is instantaneously released from a source zone of volume $\mathcal{V}_0$. Following the Lagrangian viewpoint, the solute plume is composed by a collection of particles. Such particles, originating from location $\boldsymbol{a}$ within the injection volume (i.e., $\boldsymbol{a} \in \mathcal{V}_0$), have a trajectory $\boldsymbol{X}_t$ given by the sum of the advective trajectory $\boldsymbol{X}$ and the displacement trajectory associated with local-scale dispersion $\boldsymbol{X}_d$ (e.g., Fiori & Dagan, 2000). Fiori (2001) developed a framework to quantify the value of local concentration without uncertainty. The idea is based on the assumption that the plume consists of a collection of several elementary Darcy-scale solute particles with a characteristic length small compared to the local scale but large compared to the pore scale. The trajectory of the center of mass of such Darcy-scale particle is indicated with $\boldsymbol{P}(t,\boldsymbol{m})$, where $\boldsymbol{m}$ is the initial position of the center of mass. The Lagrangian concentration, here denoted as c_L, is then defined as the projection of the local concentration in a mobile system of reference centered in $\boldsymbol{P}$, namely $\boldsymbol{\xi}=\boldsymbol{x}-\boldsymbol{P}(t,\boldsymbol{m})$. The analytical expression for c_L is given by (see Boso et al., 2013, equation (13)):

$$c_L(\boldsymbol{\xi},t|\Theta_N,\Theta_E)=C_0\prod_{i=1}^{3}\frac{1}{2}\left\{\mathrm{Erf}\left[\frac{\xi_i+L_i/2}{\sqrt{2W_{ii}(t,0|\Theta_N,\Theta_E)}}\right]-\mathrm{Erf}\left[\frac{\xi_i-L_i/2}{\sqrt{2W_{ii}(t,0|\Theta_N,\Theta_E)}}\right]\right\}, \tag{12}$$

where Erf indicates the error function, L_i is the dimension of the source zone along the ith direction, and W_{ii} are the spatial moments of $\boldsymbol{W}_t(t;\boldsymbol{a},\boldsymbol{m}|\Theta_N,\Theta_E)=\boldsymbol{X}_t(t;\boldsymbol{a}|\Theta_N,\Theta_E)-\boldsymbol{P}(t,\boldsymbol{m}|\Theta_N,\Theta_E)$, namely the trajectory of the Darcian particle in the $\boldsymbol{\xi}$ coordinate system. They represent the effective spreading with respect to the plume's centroid. The scheme adopted to define the Lagrangian concentration and the associated particle trajectory $\boldsymbol{W}_t$ is depicted in the Figure 2. Further details can be found in Fiori (2001) and are briefly recapitulated in Appendix B, which contains the analytical expressions of the moments W_{ii} for transient flow. The accuracy of equation (12) was tested against numerical simulations and field data (Boso et al., 2013).

The appealing feature of this approach is the possibility of calculating the concentration c without uncertainty for the case of a point-like injection and finite Pe. As demonstrated in Fiori (2001), under these conditions, the uncertainty of the concentration is transferred to the actual position of the plume, which is filtered out by the definition of Lagrangian concentration. The validity of the Lagrangian framework, namely

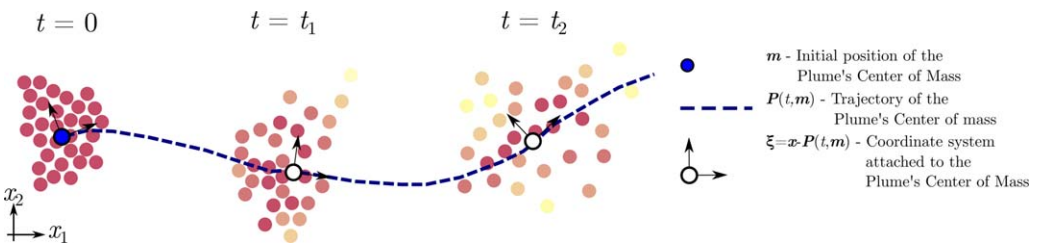

Figure 2. A sketch representing the collection of particles released within the support volume $\Delta\mathcal{V}_0$ of the measured concentration centered at $\boldsymbol{x}=\boldsymbol{m}$. The concentration is defined as $c=n_{\Delta\mathcal{V}_0}\Delta M/\Delta\mathcal{V}_0$, where $n_{\Delta\mathcal{V}_0}$ is the number of particles within $\Delta\mathcal{V}_0$ and ΔM the mass associated with the single particle. Point concentration is therefore defined by letting $\Delta\mathcal{V}_0 \to 0$. $\boldsymbol{P}(t,\boldsymbol{m})$ indicates the trajectory of the center of mass of the particles originating within the support volume $\Delta\mathcal{V}_0$ centered at $\boldsymbol{x}=\boldsymbol{m}$. The Lagrangian concentration is then defined as the projection of the local concentration c on a system of reference $\boldsymbol{\xi}$ attached to P.

equation (13), has been verified against field experiments and high resolution numerical simulations (Boso et al., 2013; de Barros et al., 2015). The Lagrangian concentration was also employed to quantify the concentration probability density function (de Barros & Fiori, 2014) and successfully compared to other existing metrics of uncertainty (Bellin & Tonina, 2007; Fiori & Dagan, 2000).

Next, using the FOA, we develop a novel semianalytical solution for the dilution index. The solution accounts for transient flow according to the model described above. By assuming that the volume of the plume is much smaller than the heterogeneity scale of K (i.e., $L_i \ll I$), see assumption 4 in section 3.1, c_L assumes the following form for an instantaneous point injection (see de Barros et al., 2015, equation (16)):

$$c_L(\xi, t|\Theta_N, \Theta_E) = C_0 \prod_{i=1}^{3} \frac{1}{\sqrt{2\pi\, W_{ii}(t, 0|\Theta_N, \Theta_E)}} \exp\left[-\frac{\xi_i^2}{2W_{ii}(t, 0|\Theta_N, \Theta_E)}\right]. \tag{13}$$

Substituting expression (13) in equation (3) yields to the entropy for solute in the Lagrangian framework. Such expression is then substituted to equation (2), leading to an analytical formulation for the dilution index (see de Barros et al., 2015, section 4):

$$E(t|\Theta_N, \Theta_E) = (2\pi)^{3/2} \exp\left(\frac{3}{2}\right) \prod_{i=1}^{3} \sqrt{W_{ii}(t, 0|\Theta_N, \Theta_E)}. \tag{14}$$

Equation (14) is the key relationship used here to investigate the coupled effect of geological structure of porous media and engineering-induced velocity fluctuation on dilution index. It quantifies the efficiency of the natural geoengineered mixer for conservative solute. It is emphasized that assuming a point-like source allows us to obtain an analytical solution for dilution index (de Barros et al., 2015). However, entropy for finite plumes can be quantified as well by numerically integrating equation (3) after replacing c with c_L provided by equation (12) (see e.g., Boso et al., 2013).

4. Illustration

In this section, we compute the dilution index for simple periodic flows with the goal of illustrating the novel semianalytical solution. Specific details related to the periodic flow field adopted in this analysis are provided in section 4.1. Subsequently, section 4.2 explores the flexibility of the semianalytical expression. For the sake of clarity, we recall the assumptions employed here: a small source zone with respect to the integral scale of Y, low-to-mild heterogeneous aquifers (i.e., $\sigma_Y^2 \lesssim 1$) and slowly varying transient flow. The effect of engineered sequences of injection and withdrawal on the flow field is assumed to be reflected in the mean hydraulic gradient and therefore in the transient mean velocity $\boldsymbol{U}(t)$. For the upcoming illustrations, we adopt an isotropic constant local-scale dispersivity α_d and the Gaussian axial-symmetric covariance model for Y defined in equation (10).

4.1. Definitions

Due to the action of multiple injection and extraction rates (see Figure 1), the solute plume is forced to spread and diffuse within a region constrained by the array of wells. In order to minimize the risk of clogging well and comply with regulatory agencies, contaminant extraction at pumping wells should be avoided. Here we assume that the unsteady flow field produced by alternate pumping is approximated by an oscillating flow field in the domain $\mathcal{W}$ in the absence of sinks or sources. Through such approximation, we are able to provide a fast and simple solution, though physically based, that accounts for the coupled effect of geoengineered fluctuations and medium heterogeneity. As a consequence, the mean trajectory $\langle \boldsymbol{X} \rangle = \Gamma$ can be described by an oscillatory model which is an approximation of the complex unsteady field resulting from the sequence of injection and extraction. For the sake of simplicity, in this work we consider an analytical 2-D closed line for the mean trajectory Γ given by

$$\Gamma(t|\Theta_E) = [A\cos(\omega_o t)\cos(\omega_f t),\ A\cos(\omega_o t)\sin(\omega_f t),\ 0], \tag{15}$$

where A is the amplitude of the oscillation and ω_o and ω_f are the angular velocities. The model provided by equation (15) ensures that the solute plume moves backward and forward at angular velocity ω_o, while it circulates with angular velocity ω_f. Although the present model can be implemented with complex 3-D expressions for Γ, in this work we adopt 2-D mean trajectory in the plane (x_1, x_2) for the sake of simplicity.

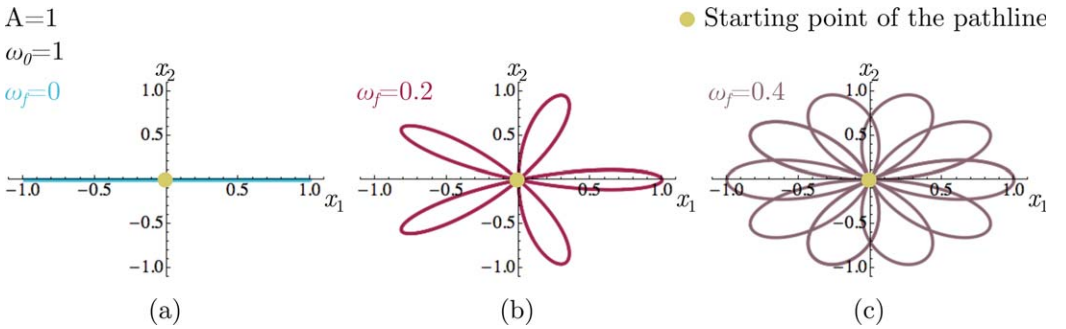

Figure 3. Closed mean trajectories Γ as a function of the angular velocity ω_f for a unitary amplitude of oscillation A and a unitary frequency of linear oscillation ω_o. The analytical expression for Γ is given by equation (15) and describes a closed 2-D pathline in the horizontal plane (x_1, x_2).

The angular velocities ω_o and ω_f refer directly on the designed technical setup, and they depend on how many wells are operating and how often they switch between injection and withdrawal. From an operational point of view, a realistic value of the oscillatory frequencies should not be larger than once in a week (Bagtzoglou & Oates, 2007), which in turn is in line with the hypothesis of slowly varying transient flow. Note that by definition $\omega_j = 2\ \pi\ \nu_j$, where ν_j is the frequency and $j = (o, f)$. Figure 3 shows a few examples of the mean flow patterns produced by equation (15). The patterns depicted in Figure 3 are computed with different values of angular velocity ω_f. The transient mean velocity $\boldsymbol{U}$, see the first line of equation (7), is thus obtained from equation (15) as follows:

$$\boldsymbol{U}(t|\Theta_E) = \frac{d\Gamma(t|\Theta_E)}{dt} = \{-A[\omega_o \sin(\omega_o t)\cos(\omega_f t) + \omega_f \cos(\omega_o t)\sin(\omega_f t)], \\ A[\omega_f \cos(\omega_o t)\cos(\omega_f t) - \omega_o \sin(\omega_o t)\sin\omega_f t], 0\}. \tag{16}$$

The magnitude of the time-averaged mean velocity, here defined as $\bar{U}$, is a function of engineered parameters and assumes the following expression:

$$\bar{U}(\Theta_E) = \frac{\omega_o}{2\pi}\int_0^{2\pi/\omega_o} U(t|\Theta_E)\, dt = \frac{2A\,\omega_o}{\pi}\left\{\mathrm{E}_{\mathrm{elliptic}}\left[1-\left(\frac{\omega_f}{\omega_o}\right)^2\right]\right\}, \tag{17}$$

where $U = |\boldsymbol{U}|$ is the L-2 norm and $\mathrm{E}_{\mathrm{elliptic}}$ indicates the complete elliptic integral defined as

$$\mathrm{E}_{\mathrm{elliptic}}[z] = \int_0^{\pi/2} \sqrt{1 - z\sin^2(\varphi)}\, d\varphi. \tag{18}$$

Equations (15) and (16) are used to calculate the moments W_{ii}, $i = (1–3)$, given by equation (B4), which are in turn substituted into equation (14) to relate the dilution index E with the designed parameters of the engineered setup. In order to generalize the results, the analysis is conducted in dimensionless form with reference to the longitudinal integral scale I (for length) and $1/\omega_o$ (for time). The relevant quantities investigated are related to the aquifer in natural conditions, represented by $\Theta_N = (Pe, \sigma_Y^2, e)$, and to the engineered sequence of injection and withdrawal, represented by $\Theta_E = (\lambda, \Omega)$, where $\lambda = A/I$ is the normalized amplitude of the engineered pumping scheme and $\Omega = \omega_f/\omega_o$ is the ratio between the two angular velocities. It is highlighted that λ determines the spatial arrangement of the array of wells, whereas Ω is an operational parameter controlled by the designed injection-extraction schedule.

4.2. Coupled Effects of Θ_N and Θ_E on Dilution

Next we systematically illustrate the impact of the parameters $\Theta_N = (Pe, \sigma_Y^2, e)$ and $\Theta_E = (\lambda, \Omega)$ on the temporal evolution of the dilution index E.

Figure 4 shows the combined effect of the oscillation amplitude λ (in the longitudinal direction) and oscillation ratio Ω on the dilution index E. The inset of Figure 4 shows the ratio between E and E_N. The latter indicates the dilution index for a unidirectional and steady mean flow. To compare the results with the dilution index under engineering-induced conditions, E_N is calculated by assuming a mean flow with magnitude given by equation

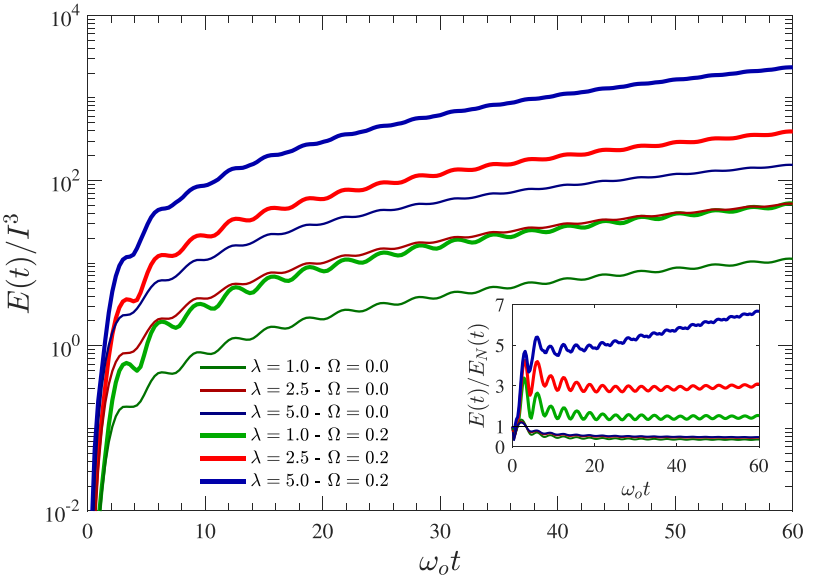

Figure 4. Temporal evolution of dilution index E for several coupled values of dimensionless oscillation amplitude λ and oscillation ratio Ω. The inset represents the ratio E/E_N as a function of time. E_N is defined as the dilution index for a steady and unidirectional flow. The other parameters used during the computation are $\sigma_Y^2 = 0.5$, $e = 0.1$ and $Pe = 10^3$.

(17). The results are computed for the following set of parameters: $\sigma_Y^2 = 0.5$, $e = 0.1$ and $Pe = 10^3$. The oscillation amplitude λ epitomizes the distance between the operating wells, thereby indicating the space in which the plume is constrained. The mixing efficiency increases significantly with λ; in fact larger values of λ entail that the plume experiences more heterogeneity of the flow field, which increases dilution. On the other hand, the injection-extraction setup operates as a system of plume containment, preventing the migration of the contaminant to the surrounding clean groundwater. The figure inset shows that, when compared to transport under natural gradient (i.e., uniform-in-mean flow), the dilution of a plume is reduced when the amplitude of the oscillation λ decreases. In other words, the price to pay for the containment within a geoengineered flow field is a smaller dilution with respect to the case of a uniform mean flow. Therefore the optimal design of λ is the result of a trade-off between obtaining a larger dilution and constraining the plume within a smaller volume.

The parameter Ω encases the operational scheme of mean flow alternation and is defined by the ratio between the two angular velocities ω_o and ω_f. In other words, it is the factor controlling the different geometry of the mean trajectory Γ (see Figure 3). For example, the closed mean trajectory Γ obtained by setting $\Omega = 0.0$ and $\Omega = 0.2$ are shown in Figures 3a and 3b, respectively. By increasing Ω, the system of alternate pumping induces a circulation pattern on the solute plume trajectory, leading to braiding paths. The resulting alternation of shear and strain increases the time needed for the plume to travel the entire closed path while simultaneously sampling the variability of the aquifer's hydraulic properties. As a consequence of the longer mean path, the plume samples more heterogeneity which, in combination with the alternation of shear and strain, enhances plume's deformation and therefore dilution (see detailed discussion in de Barros et al., 2012). As can be seen from the insert of Figure 4, the semianalytical results show that the fluctuating, but oscillating, mean flow may lead to more dilution when compared to the unidirectional and steady mean flow. Thus, the aforementioned limitations of containment can be overcome by introducing oscillations and circulation in the closed pathline. Similar results have been obtained numerically by Neupauer et al. (2014) and subsequent studies by using the theory of chaotic advection.

Furthermore, Figure 4 shows fluctuations in the dilution index that are produced by the alternate compaction and extension of the plume. Such behavior is induced by the back-and-forth movement with angular velocity ω_o, which epitomizes the alternation of extraction and injection. As observed by Rodríguez-Escales et al. (2017), entropy reduces during the compaction stage of the solute plume, while it increases again during expansion, leading to the oscillating behavior shown in Figure 4.

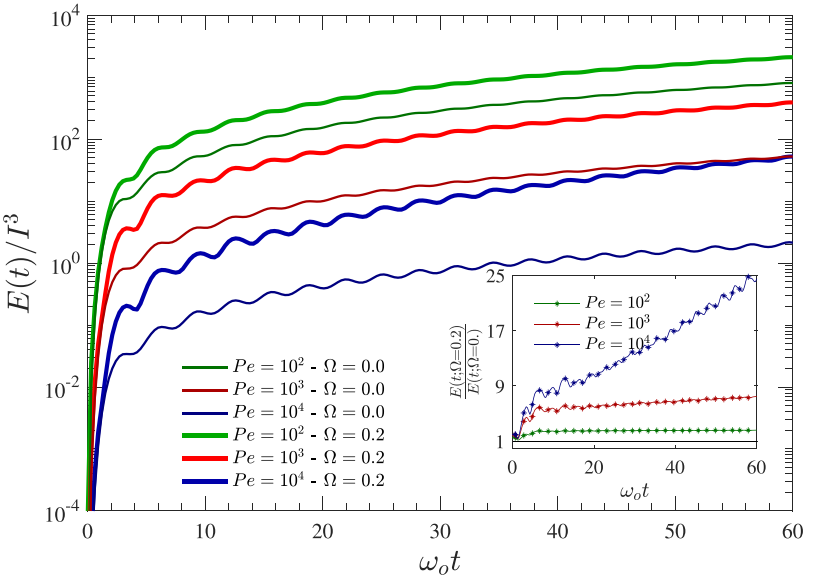

Figure 5. Coupled effect of *Pe* and oscillation ratio Ω on dilution index *E*. The inset shows $E(t;\Omega{=}0.2)/E(t;\Omega{=}0.0)$ as a function of time for several value of *Pe*. The results are calculated by considering $\lambda{=}2.5$, $\sigma_Y^2{=}0.5$ and $e = 0.1$.

Figure 5 illustrates the coupled effect of *Pe* and Ω on diluting the point-like source for an aquifer characterized by $\sigma_Y^2{=}0.5$ and $e = 0.1$. The mean velocity has a longitudinal oscillation with amplitude $\lambda = 2.5$. As expected, *Pe* has a significant effect on transport. Changing the *Pe* by two orders of magnitude, which correspond to the values typically found in the field (see Adams & Gelhar, 1992; Freyberg, 1986; Garabedian et al., 1991), leads to an increase of three orders of magnitude on the dilution index. When $Pe = 10^4$ (blue lines in Figure 5), transport can be considered purely advective, which results in visible oscillatory fluctuations in the time series of the dilution index. By decreasing *Pe*, the role of local-scale dispersion mechanisms in attenuating concentration variability becomes more significant and therefore, the temporal oscillations in the dilution index are smoothed out. The inset of Figure 5 depicts the ratio $E(t;\Omega = 0.2)/E(t;\Omega = 0.0)$ for several values of *Pe*. Such ratio indicates the dilution efficiency obtained by changing Ω (i.e., using different pumping schedule) with the same λ (i.e., the spatial arrangement of the array of wells). As shown by the inset, dilution becomes progressively independent of the oscillation ratio Ω with decreasing *Pe*. In other words, local-scale dispersion attenuates the effect of engineering-induced fluctuations on dilution. Conversely, if transport is dominated by advection, dilution is more sensitive to the pumping scheme represented by Ω. From a practical point of view, *Pe* may be considered the key parameter controlling the efficiency of a designed setup of extraction-injection wells.

Figure 6 shows the sensitivity of the dilution index to different level of aquifer heterogeneity (epitomized by σ_Y^2) coupled to several values of oscillation ratio. The results in Figure 6 are computed for $\lambda = 2.5$, $e = 0.1$ and $Pe = 10^3$. The mixing efficiency increases with medium heterogeneity σ_Y^2, since dilution is controlled by the interplay between large-scale advection and local-scale dispersion (compare the curve obtained for $\sigma_Y^2 = 0.1$ with $\sigma_Y^2{=}0.8$) . Higher values of σ_Y^2 lead to a stronger deformation of the plume. This deformation increases local concentration gradients, thereby enhancing mass transfer, which is the main mechanism inducing dilution. Notice that local dispersion has counteracting effects on mass flux: according to Fick's law, an increase of local-scale dispersion leads to a larger local mass flux, which is however contrasted by the consequent reduction of the concentration gradient. This leads to a saturation effect with the rate of increase of the dilution index that attenuates with increasing σ_Y^2. This effect has been observed by Boso and Bellin (2012) for a uniform mean flow and is not observed here, due to the limited variability of σ_Y^2 required by the FOA employed in this work. The temporal oscillations observed in Figure 6 indicate that the solute plume is stretched and compressed continuously due to the imposed temporal fluctuations in the mean flow (which in this work mimics the fluctuation generated by alternate pumping). Such oscillating behavior of the dilution index in time becomes more evident as the heterogeneity of the aquifer increases (i.e., larger σ_Y^2). As shown in the inset of Figure 6, the ratio $E(t;\ \Omega = 0.2)/E(t;\ \Omega = 0.0)$ increases with σ_Y^2, thereby

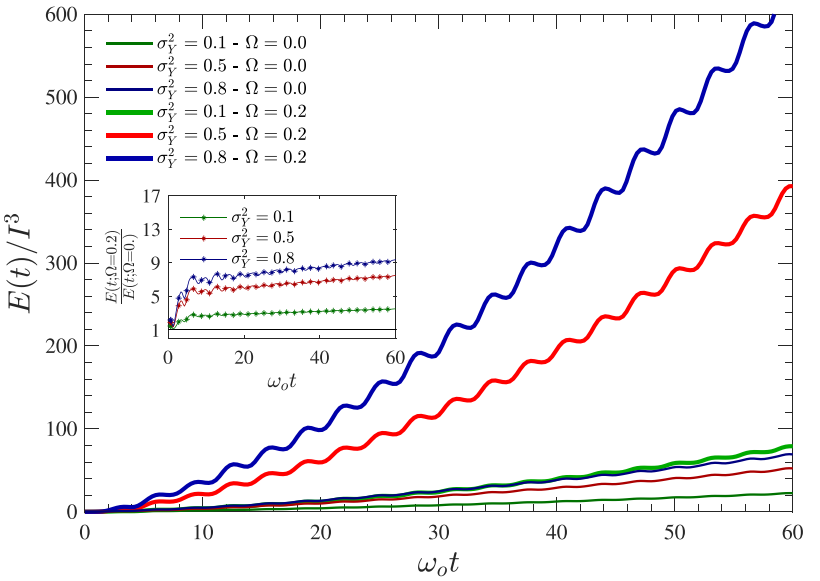

Figure 6. The effect of log-conductivity variance σ_Y^2 combined with oscillation ratio Ω on dilution index E. The inset depicts the ratio $E(t; \Omega = 0.2)/E(t; \Omega = 0.0)$ for several values of log-conductivity variance. The computation is carried with the following parameters: λ=2.5, $e = 0.1$ and $Pe = 10^3$.

indicating that the medium heterogeneity enhances the effect of the injection-extraction scheme on dilution. On the other hand, higher heterogeneity triggers also the appearance of fast flow channels, by which the contaminant could unexpectedly reach the pumping wells. Such event might clog the well through mineral precipitation and biomass growth, and cause regulatory concern, if the engineered system requires reinjection (Neupauer et al., 2014).

Next, we explore the impact of the statistical anisotropy ratio e on plume dilution in the presence of temporal fluctuations. Figure 7 shows that the dilution index increases with the decrease of e. For smaller values of e, the geological formation resembles more anisotropic (e.g., stratified) media. As a result, the vertical characteristic length of the plume scales with I_V (e.g., Gelhar & Axness, 1983; Matheron & De Marsily, 1980;

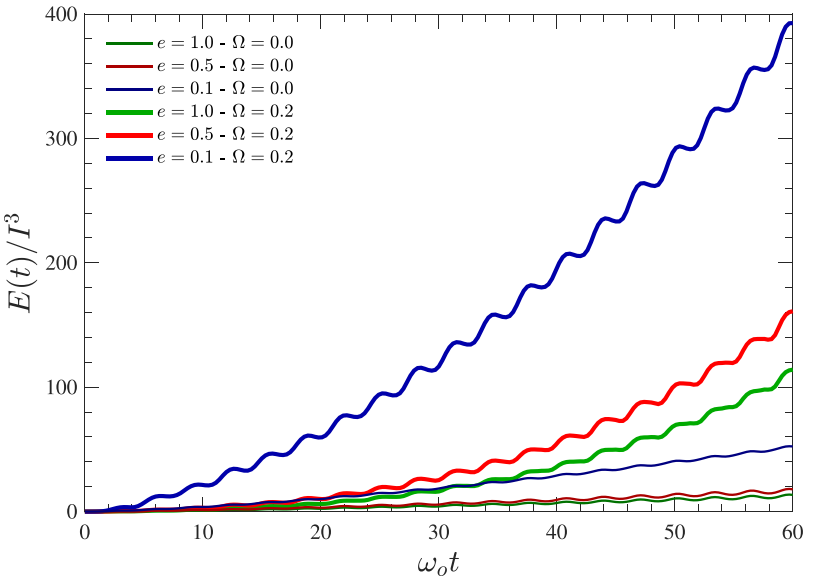

Figure 7. Dilution index as a function of time for several values of anisotropy ratio e and oscillation ratio Ω. The results are computed for λ=2.5, σ_Y^2=0.5 and $Pe = 10^3$.

Neuman et al., 1987) and the plume dilutes quicker. Similar observations are reported in de Barros and Fiori (2014) where the authors relate the shape of the concentration cumulative distribution function with dilution for several values of *e*.

5. Application to the Cape Cod Site

In this section we demonstrate the capability of the proposed engineered-induced transient flow to enhance dilution with respect to natural flow conditions. For this purpose, we chose the shallow aquifer at Cape Cod, Massachussetts (USA). Starting from July 1985, this site has been object of a large-scale natural-gradient tracer test campaign (LeBlanc et al., 1991), which has produced a large volume of geostatistical studies reported in the literature (e.g., Fitts, 1996; Garabedian et al., 1991; Hess et al., 1992). The conditions and the features that characterize such contaminated site are rather different from the assumptions at the basis of our model. However, our goal here is not to discuss a rigorous application of engineered injection and extraction for remediation, but rather to illustrate a simple application of the model and its potential to reduce the remediation time of a contaminated aquifer by enhancing dilution.

The Cape Cod aquifer is weakly heterogeneous with a mean uniform velocity of $U_N = 0.42$ m/d under natural conditions. The analysis of the spatial variability of the *Y*-field leads to normally distributed RSF with variance $\sigma_Y^2 = 0.24$. The structure of the *Y*-field is characterized by integral scales of $I = 3.5$ m and $I_V = 0.19$ m in the longitudinal and vertical directions, respectively, leading to an anisotropy ratio of $e = 0.054$ (Garabedian et al., 1991; Hess et al., 1992). Furthermore, we assumed the local-scale dispersivity isotropic and equal to $\alpha_d = 0.5$ mm. Such value was inferred by Fiori and Dagan (1999) on the basis of the analysis conducted by Fitts (1996) and has been adopted in several following works (Boso et al., 2013; de Barros et al., 2015; Fiori, 2001, 2003).

We assume the plume as instantaneously injected and small compared to the heterogeneity scale. The dilution index was determined by substituting the moments W_{ii}, $i = (1–3)$, provided by equation (B1), into the expression (14) for several engineered transient flow schemes and with the above aquifer's parameters (i.e., $\sigma_Y^2 = 0.24$, $I = 3.5$ m, $e = 0.054$, $\alpha_d = 0.5$ mm). Flow configurations are varied by changing the oscillation amplitude A and the angular velocities ω_o and ω_f . We recall that A is related to the physical distance between the wells, while ω_o and ω_f depend on the number of operating wells and the pumping schedule. Reasonable values of ω_o and ω_f are limited by operational constraints and range between week^{-1} and year^{-1} (Bagtzoglou & Oates, 2007). To ensure a fair comparison among the pumping schemes, we select the engineering parameters such that to obtain a time-averaged mean velocity equal to the natural mean velocity of the aquifer, i.e., $\bar{U}(A, \omega_o, \omega_f) \equiv U_N$. In this way, we consider the same *Pe* for all cases and the engineering parameters are in the range of realistic values. The values of these parameters are provided in the legend of Figure 8, which illustrates the behavior of the dilution index for the natural-gradient and the engineering-induced transient flows schemes.

The black dashed line indicates the dilution index for the aquifer under natural head gradient. As already discussed in section 4.2, the back-and-forth schemes (see green and blue lines of Figure 8) lead to a dilution smaller than the steady flow case under natural conditions. In such a case, the plume experiences alternate expansion and contraction, which reduces transverse mass flux with respect to the natural-gradient condition. However, dilution can be enhanced by increasing ω_f, i.e., inducing a forced circulation. The circulation component in the mean flow, in combination with the oscillatory one, causes larger plume deformations, which in turn enhances dilution. In this way, one can at the same time contain the plume and increase dilution, thereby enhancing attenuation of plume concentration. At early times, the circulating scheme with larger frequencies and smaller A (see the orange line) is the more efficient configuration, though slightly. After about $t = 150$ days, a larger dilution is induced by the circulating scheme with larger amplitude A but smaller frequencies (the red line). Notice that time window of 150 days is slightly less than the time needed to complete a full revolution of the red scheme ($T_{period} = 2\pi/\omega_o = 183$ days).

Based on the above results, we provide in the following some engineering design recommendations. The first step is to define the distance between the wells, which corresponds to the maximum possible oscillation amplitude A. Such value depends on the physical constraints of the site (e.g., boundaries or sensitive targets). Subsequently, the best set of engineering parameters is selected as function of the operational and technical constraints. On the basis of the computational results, we suggest to choose larger

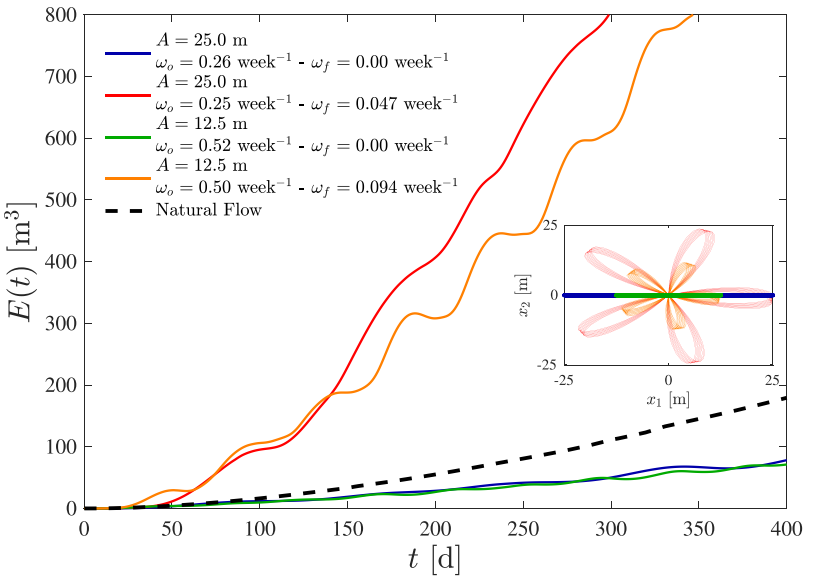

Figure 8. Application to the Cape Cod site: the temporal behavior of dilution index for engineering-induced transient flow of oscillation. The combinations of engineering parameters ensure realistic values of the time-averaged velocity, which is assumed equal the natural mean velocity of the aquifer U_N.

frequencies at the early stages and increase the oscillation amplitude (i.e., by decreasing the frequencies) with the time. Although such flow configurations can only be approximated in the field practice, we emphasize that circulating oscillating flow is to be preferred.

6. Summary

This work conceptualizes the subsurface formation as a geoengineered natural mixer, in analogy to mechanical mixing tanks (e.g., Paul et al., 2004). Following the ideas of Neupauer et al. (2014, and references therein), we explore how natural heterogeneity and temporal fluctuations induced by external factors (such as engineered injection and extraction) influence the mixing behavior of the solute plume. As opposed to previous works, we tackle the problem utilizing analytical tools in a 3-D setting. To this end, we obtain a semianalytical solution for the temporal evolution of the dilution index, while accounting for parameters characterizing both the natural heterogeneity of subsurface formation and the temporal oscillatory features of the 3-D flow field.

Due to its analytical features, the present model allows to systematically investigate the joint impact of the geological properties of the 3-D aquifer and the engineered design of flow fluctuations (such as the ones produced by the system of alternate pumping) on the overall plume mixing behavior. To achieve this goal, we expand the solution of the dilution index derived in de Barros et al. (2015) to transient flows. Our model relies on the assumptions listed in section 3.1. In short, the accuracy of our solution is limited to weak heterogeneity and small sources (compared to the heterogeneity scale). Furthermore, the unsteady flow field is modeled by a slowly oscillating mean flow field in the absence of sources or sinks. The solution methodology is based on the Lagrangian concentration concept developed by Fiori (2001).

Our results confirm (analytically) the impact of the hydraulic conductivity structure on mixing, as already observed for steady flow fields in previous works. As expected, solute dilution is strongly enhanced by heterogeneity of hydraulic conductivity and local-scale dispersion. Several schedules of alternate pumping were analyzed as a function of the oscillation amplitude (which refers to the physical distance between the wells) and two angular velocities (which account for the rates and duration of injection-extraction). We point out that the two angular velocities, ω_o and ω_f, describe linear oscillation and rotation, respectively. The results suggest that inducing forced circulation in the mean trajectory, i.e., increasing ω_f, together with natural heterogeneity, contributes to augment dilution. On the other hand, local-scale dispersion attenuates

the effect of induced temporal fluctuations on dilution. In fact, when *Pe* decreases, the main transport mechanism becomes dispersion and the transport effects originating from advection are overwhelmed. These features should be carefully taken in account when designing such in situ treatment systems.

The capabilities of the proposed semianalytical model are illustrated by a simple application to the Cape Cod site. We compare several patterns of alternate flow. The engineering parameters are chosen so that the related time-averaged mean velocity is the same for all the schemes. The results confirm that dilution is augmented by circulating flows, obtained by inducing forced oscillation in both longitudinal and lateral directions.

It is highlighted that the proposed semianalytical model neglects storage effect related to medium and fluid compressibility (i.e., the storage coefficient S_s is assumed to be very small and therefore negligible). Thus, changes in the configuration of the flow field, triggered by changes in the pumping schedule at the wells, propagate instantaneously to the entire domain and the flow can be considered as a succession of steady states. As a result, the dilution index is proportional to ω_o, which is a realistic approximation only for small oscillation frequency. We surmise that a fully transient flow solution, i.e., after assuming $S_s \neq 0$, would lead to an optimum frequency of oscillation, which however would be likely limited by technical and operational constraints (Bagtzoglou & Oates, 2007).

The results presented in this work showed analytically that engineering-induced transient flow can significantly enhance dilution, thereby helping to improve groundwater management practices and perform an efficient plume containment. It is emphasized that the analytical features of the model enable to efficiently screen alternative flow configurations and alleviate the computational burden. In addition the present framework can provide a robust benchmark for more sophisticated numerical models, providing that the above assumptions are satisfied.

Appendix A: Derivation of the First-Order Approximation of the Velocity Covariance Function

Equation (7) is first transformed in the Fourier space:

$$\hat{\boldsymbol{u}}(\boldsymbol{k},t)=\frac{K_G}{n}\left[\boldsymbol{J}(t|\Theta_E)\hat{Y}'(\boldsymbol{x}|\Theta_N)-\imath\boldsymbol{k}\hat{h}(\boldsymbol{k},t|\Theta_N,\Theta_E)\right], \tag{A1}$$

where $\boldsymbol{k}=(k_1,k_2,k_3)$ is the wave number vector with $k=|\boldsymbol{k}|$ its L-2 norm, $\imath$ is the imaginary unity, the hat $\hat{}$ indicates the Fourier transform. Similarly, equation (8) assumes the following expression in Fourier space:

$$\hat{h}(\boldsymbol{k},t|\Theta_N,\Theta_E)=-\imath\frac{\boldsymbol{J}(t|\Theta_E)\cdot\boldsymbol{k}}{k^2}\hat{Y}'(\boldsymbol{k}|\Theta_N). \tag{A2}$$

By substituting (A2) into (A1), we obtain the following first-order approximation of the Fourier transform for the velocity:

$$\hat{\boldsymbol{u}}(\boldsymbol{k},t|\Theta_N,\Theta_E)=\frac{K_G}{n}\hat{Y}'(\boldsymbol{k}|\Theta_N)\left[\boldsymbol{J}(t|\Theta_E)-\boldsymbol{k}\frac{\boldsymbol{J}(t|\Theta_E)\cdot\boldsymbol{k}}{k^2}\right], \tag{A3}$$

which is substituted into the expression of the Fourier transform of the velocity covariance function:

$$\hat{u}_{ij}(\boldsymbol{k},t',t''|\Theta_N,\Theta_E)=\langle\hat{u}_i(\boldsymbol{k},t'|\Theta_N,\Theta_E)\,\hat{u}_j(\boldsymbol{k},t''|\Theta_N,\Theta_E)\rangle. \tag{A4}$$

The above expression leads to the final expression (9). Notice that for a unidirectional steady state mean velocity field, i.e., $\boldsymbol{U}(t)=(U,0,0)$, equation (9) reduces to the well known first-order approximation (Dagan, 1989):

$$\hat{u}_{ij}(\boldsymbol{k})=U^2\left[\delta_{i1}-\frac{k_i k_1}{k^2}\right]\left[\delta_{j1}-\frac{k_j k_1}{k^2}\right]\hat{C}_Y(\boldsymbol{k}). \tag{A5}$$

Appendix B: Statistical Moments of the Particle Trajectories

By applying the first-order approximation, namely assuming a linear dependence between velocity fluctuations $\boldsymbol{u}$ and the log-conductivity field fluctuations Y', the advective trajectories $\boldsymbol{X}$ are normally distributed

(details are provided in Fiori & Dagan, 2000). As a consequence, the trajectory $\boldsymbol{W}$ has a multinormal distribution, which is therefore fully characterized by the first and the second moments (for additional details see Fiori, 2001):

$$\begin{aligned}&\langle \boldsymbol{W}_t(t,\boldsymbol{a},\boldsymbol{m}|\Theta_N,\Theta_E)\rangle = \boldsymbol{a}-\boldsymbol{m},\\ &W_{ii}(t,\boldsymbol{a}-\boldsymbol{m}|\Theta_N,\Theta_E)=\langle W'_{t,i}(t,\boldsymbol{a},\boldsymbol{m}|\Theta_N,\Theta_E)W'_{t,i}(t,\boldsymbol{a},\boldsymbol{m}|\Theta_N,\Theta_E)\rangle = \\ &\quad = X_{ii}(t|\Theta_N,\Theta_E)+X_{d,ii}(t|\Theta_N,\Theta_E)+Z_{ii}(t;0)-2Z_{ii}(t,\boldsymbol{a}-\boldsymbol{m}|\Theta_N,\Theta_E),\end{aligned} \tag{B1}$$

with $i=(1\text{–}3)$. X_{ii} and $X_{d,ii}$ are the one particle auto-covariances of the the advective and local-scale displacements, respectively, and Z_{ii} is the two-particle trajectory cross-covariance. In an unsteady flow field, the covariance $X_{d,ii}$ is a function of the time-dependent mean flow, as follows (see Indelman & Dagan, 1999, equation (28)):

$$X_{d,ii}(t|\Theta_N,\Theta_E)=2\alpha_d\int_0^t U(t'|\Theta_E)\,dt'=2\alpha_d\chi(t|\Theta_E), \tag{B2}$$

where α_d is the local-scale dispersivity and $\chi(t|\Theta_E)=\int_0^t U(t'|\Theta_E)\,dt'$. The latter has an analytical expression obtained by substituting equation (16) and integrating, as follows:

$$\begin{aligned}\chi(t|\Theta_E) \quad &= \int_0^t U(t'|\Theta_E)\,dt' = \\ &= \lambda\left\{\Omega\,\mathrm{E}_{\mathrm{elliptic}}\left[\pi\mathcal{F}\left(\frac{\omega_o}{\pi}t\right)|\frac{\Omega^2-1}{\Omega^2}\right]+2\,\mathrm{E}_{\mathrm{elliptic}}\left(1-\Omega^2\right)\mathcal{I}\left(\frac{\omega_o}{\pi}t\right)\right\},\end{aligned} \tag{B3}$$

where $\mathrm{E}_{\mathrm{elliptic}}(\cdot)$ and $\mathrm{E}_{\mathrm{elliptic}}(\cdot|\cdot)$ indicate the complete and incomplete elliptic integral, respectively, and $\mathcal{I}(z)$ and $\mathcal{F}(z)$ represent the integer part and fractional part of the number z, respectively.

By assuming a point-like injection, i.e., for the limit $|\boldsymbol{a}-\boldsymbol{m}|\to 0$, W_{ii} in equation (B1) can be further simplified to

$$W_{ii}(t,0|\Theta_N,\Theta_E)=X_{ii}(t|\Theta_N,\Theta_E)+X_{d,ii}(t|\Theta_N,\Theta_E)-Z_{ii}(t;0|\Theta_N,\Theta_E). \tag{B4}$$

Under the hypothesis of a point source and low heterogeneity, the moments of the particle X_{ii} and Z_{ii} in equation (B4) assume the following values (Fiori & Dagan, 2000):

$$\begin{aligned}X_{ii}(t|\Theta_N,\Theta_E)= \quad &\frac{1}{(2\pi)^{3/2}}\int_0^t\int_0^t\int\hat{u}_{ii}(\boldsymbol{k},t|\Theta_N,\Theta_E)\exp\{-\imath\boldsymbol{k}\cdot[\Gamma(t_1|\Theta_E)-\Gamma(t_2|\Theta_E)]+\\ &-k^2\alpha_d\mathrm{Abs}[\chi(t_1|\Theta_N,\Theta_E)-\chi(t_2|\Theta_N,\Theta_E)]\}\,d\boldsymbol{k}\,dt_1\,dt_2,\end{aligned} \tag{B5}$$

$$\begin{aligned}Z_{ii}(t;0|\Theta_N,\Theta_E)= \quad &\frac{1}{(2\pi)^{3/2}}\int_0^t\int_0^t\int\hat{u}_{ii}(\boldsymbol{k},t|\Theta_N,\Theta_E)\exp\{-\imath\boldsymbol{k}\cdot[\Gamma(t_1|\Theta_E)-\Gamma(t_2|\Theta_E)]+\\ &-k^2\alpha_d[\chi(t_1|\Theta_N,\Theta_E)+\chi(t_2|\Theta_N,\Theta_E)]\}\,d\boldsymbol{k}\,dt_1\,dt_2,\end{aligned} \tag{B6}$$

where $\boldsymbol{k}$ is wave number and $k=|\boldsymbol{k}|$ is its L-2 norm. The function $\Gamma(t)$ is given by equation (15), $\chi(t)$ is defined in equation (B3) and $\hat{u}_{ii}(\boldsymbol{k},t)$ is the Fourier transform of the velocity covariance, which is given by equation (9).

Acknowledgments
The authors would like to thank the anonymous reviewers for their insightful comments and suggestions that have contributed to improve this paper. M.D.D. and A.B. acknowledge the support by the European Union FP7 Collaborative Research Project GLOBAQUA (Managing the effects of multiple stressors on aquatic ecosystems under water scarcity, grant 603629). All data for this paper are properly cited and referred to in the reference list.

References

Adams, E. E., & Gelhar, L. W. (1992). Field study of dispersion in a heterogeneous aquifer: 2. Spatial moments analysis. *Water Resources Research*, *28*(12), 3293–3307. https://doi.org/10.1029/92WR01757

Bagtzoglou, A. C., & Oates, P. M. (2007). Chaotic advection and enhanced groundwater remediation. *Journal of Materials in Civil Engineering*, *19*(1), 75–83. https://doi.org/10.1061/(ASCE)0899-1561(2007)19:1(75)

Bellin, A., Dagan, G., & Rubin, Y. (1996). The impact of head gradient transients on transport in heterogeneous formations: Application to the Borden site. *Water Resources Research*, *32*(9), 2705–2713. https://doi.org/10.1029/96WR01629

Bellin, A., Salandin, P., & Rinaldo, A. (1992). Simulation of dispersion in heterogeneous porous formations: Statistics, first-order theories, convergence of computations. *Water Resources Research*, *28*(9), 2211–2227. https://doi.org/10.1029/92WR00578

Bellin, A., & Tonina, D. (2007). Probability density function of non-reactive solute concentration in heterogeneous porous formations. *Journal of Contaminant Hydrology*, *94*(1), 109–125. https://doi.org/10.1016/j.jconhyd.2007.05.005

Benekos, I. D., Cirpka, O. A., & Kitanidis, P. K. (2006). Experimental determination of transverse dispersivity in a helix and a cochlea. *Water Resources Research*, *42*, W07406. https://doi.org/10.1029/2005WR004712

Boso, F., & Bellin, A. (2012). Mixing processes in highly heterogeneous formations. In *Models—Repositories of knowledge, Proceedings of ModelCARE2011* (Vol. 355, pp. 217–222). Wallingford, Oxfordshire, UK: IAHS Publication.
Boso, F., de Barros, F. P. J., Fiori, A., & Bellin, A. (2013). Performance analysis of statistical spatial measures for contaminant plume characterization toward risk-based decision making. *Water Resources Research*, *49*, 3119–3132. https://doi.org/10.1002/wrcr.20270
Bredehoeft, J. (1992). Much contaminated ground water can't be cleaned up. *Ground Water*, *30*(6), 834–835. https://doi.org/10.1111/j.1745-6584.1992.tb01564.x
Cardiff, M., Bakhos, T., Kitanidis, P. K., & Barrash, W. (2013). Aquifer heterogeneity characterization with oscillatory pumping: Sensitivity analysis and imaging potential. *Water Resources Research*, *49*, 5395–5410. https://doi.org/10.1002/wrcr.20356
Cardiff, M., & Barrash, W. (2015). Analytical and semi-analytical tools for the design of oscillatory pumping tests. *Ground Water*, *53*(6), 896–907. https://doi.org/10.1111/gwat.12308
Chang, L.-C., Shoemaker, C. A., & Liu, P. L.-F. (1992). Optimal time-varying pumping rates for groundwater remediation: Application of a constrained optimal control algorithm. *Water Resources Research*, *28*(12), 3157–3173. https://doi.org/10.1029/92WR01685
Cirpka, O. A., & Attinger, S. (2003). Effective dispersion in heterogeneous media under random transient flow conditions. *Water Resources Research*, *39*(9), 1257. https://doi.org/10.1029/2002WR001931
Cirpka, O. A., Rolle, M., Chiogna, G., de Barros, F. P. J., & Nowak, W. (2012). Stochastic evaluation of mixing-controlled steady-state plume lengths in two-dimensional heterogeneous domains. *Journal of Contaminant Hydrology*, *138*, 22–39. https://doi.org/10.1016/j.jconhyd.2012.05.007
Dagan, G. (1989). *Flow and transport in porous formations*. Berlin, Germany: Springer.
Dagan, G., Bellin, A., & Rubin, Y. (1996). Lagrangian analysis of transport in heterogeneous formations under transient flow conditions. *Water Resources Research*, *32*(4), 891–899. https://doi.org/10.1029/95WR02497
Dagan, G., & Rabinovich, A. (2014). Oscillatory pumping wells in phreatic, compressible, and homogeneous aquifers. *Water Resources Research*, *50*, 7058–7066. https://doi.org/10.1002/2014WR015454
de Barros, F. P. J., Dentz, M., Koch, J., & Nowak, W. (2012). Flow topology and scalar mixing in spatially heterogeneous flow fields. *Geophysical Research Letters*, *39*, L08404. https://doi.org/10.1029/2012GL051302
de Barros, F. P. J., Fernández-Garcia, D., Bolster, D., & Sanchez-Vila, X. (2013). A risk-based probabilistic framework to estimate the endpoint of remediation: Concentration rebound by rate-limited mass transfer. *Water Resources Research*, *49*, 1929–1942. https://doi.org/10.1002/wrcr.20171
de Barros, F. P. J., & Fiori, A. (2014). First-order based cumulative distribution function for solute concentration in heterogeneous aquifers: Theoretical analysis and implications for human health risk assessment. *Water Resources Research*, *50*, 4018–4037. https://doi.org/10.1002/2013WR015024
de Barros, F. P. J., Fiori, A., Boso, F., & Bellin, A. (2015). A theoretical framework for modeling dilution enhancement of non-reactive solutes in heterogeneous porous media. *Journal of Contaminant Hydrology*, *175–176*, 72–83. https://doi.org/10.1016/j.jconhyd.2015.01.004
Dentz, M., Borgne, T. L., Englert, A., & Bijeljic, B. (2011). Mixing, spreading and reaction in heterogeneous media: A brief review. *Journal of Contaminant Hydrology*, *120–121*, 1–17. https://doi.org/10.1016/j.jconhyd.2010.05.002
Dentz, M., & Carrera, J. (2005). Effective solute transport in temporally fluctuating flow through heterogeneous media. *Water Resources Research*, *41*, W08414. https://doi.org/10.1029/2004WR003571
Dentz, M., & de Barros, F. P. J. (2015). Mixing-scale dependent dispersion for transport in heterogeneous flows. *Journal of Fluid Mechanics*, *777*, 178–195. https://doi.org/10.1017/jfm.2015.351
Environmental Protection Agency. (1998). *Field applications of in situ remediation technologies: Chemical oxidation*. Washington, DC: Author.
Farrell, D., Woodbury, A., Sudicky, E., & Rivett, M. (1994). Stochastic and deterministic analysis of dispersion in unsteady flow at the Borden tracer-test site, Ontario, Canada. *Journal of Contaminant Hydrology*, *15*(3), 159–185. https://doi.org/10.1016/0169-7722(94)90023-X
Fiori, A. (2001). The lagrangian concentration approach for determining dilution in aquifer transport: Theoretical analysis and comparison with field experiments. *Water Resources Research*, *37*(12), 3105–3114. https://doi.org/10.1029/2001WR000228
Fiori, A. (2003). An asymptotic analysis for determining concentration uncertainty in aquifer transport. *Journal of Hydrology*, *284*(1), 1–12. https://doi.org/10.1016/S0022-1694(02)00416-X
Fiori, A., & Dagan, G. (1999). Concentration fluctuations in transport by groundwater: Comparison between theory and field experiments. *Water Resources Research*, *35*(1), 105–112. https://doi.org/10.1029/98WR01862
Fiori, A., & Dagan, G. (2000). Concentration fluctuations in aquifer transport: A rigorous first-order solution and applications. *Journal of Contaminant Hydrology*, *45*(1–2), 139–163. https://doi.org/10.1016/S0169-7722(00)00123-6
Fitts, C. R. (1996). Uncertainty in deterministic groundwater transport models due to the assumption of macrodispersive mixing: Evidence from the Cape Cod (Massachusetts, U.S.A.) and Borden (Ontario, Canada) tracer tests. *Journal of Contaminant Hydrology*, *23*(1), 69–84. https://doi.org/10.1016/0169-7722(95)00101-8
Freeze, R. A., & Cherry, J. A. (1979). *Groundwater* (604 pp.). Englewood Cliffs, NJ: Prentice Hall.
Freyberg, D. L. (1986). A natural gradient experiment on solute transport in a sand aquifer: 2. Spatial moments and the advection and dispersion of nonreactive tracers. *Water Resources Research*, *22*(13), 2031–2046. https://doi.org/10.1029/WR022i013p02031
Garabedian, S. P., LeBlanc, D. R., Gelhar, L. W., & Celia, M. A. (1991). Large-scale natural gradient tracer test in sand and gravel, Cape Cod, Massachusetts: 2. Analysis of spatial moments for a nonreactive tracer. *Water Resources Research*, *27*(5), 911–924. https://doi.org/10.1029/91WR00242
Gelhar, L. W., & Axness, C. L. (1983). Three-dimensional stochastic analysis of macrodispersion in aquifers. *Water Resources Research*, *19*(1), 161–180. https://doi.org/10.1029/WR019i001p00161
Haley, J. L., Hanson, B., Enfield, C., & Glass, J. (1991). Evaluating the effectiveness of ground water extraction systems. *Ground Water Monitoring & Remediation*, *11*(1), 119–124. https://doi.org/10.1111/j.1745-6592.1991.tb00358.x
Hess, K. M., Wolf, S. H., & Celia, M. A. (1992). Large-scale natural gradient tracer test in sand and gravel, Cape Cod, Massachusetts: 3. Hydraulic conductivity variability and calculated macrodispersivities. *Water Resources Research*, *28*(8), 2011–2027. https://doi.org/10.1029/92WR00668
Indelman, P., & Dagan, G. (1999). Solute transport in divergent radial flow through heterogeneous porous media. *Journal of Fluid Mechanics*, *384*, 159–182. https://doi.org/10.1017/S0022112098004078
Johnson, C. R., Greenkorn, R. A., & Woods, E. G. (1966). Pulse-testing: A new method for describing reservoir flow properties between wells. *Journal of Petroleum Technology*, *18*(12), 1–599. https://doi.org/10.2118/1517-PA
Jones, S. W., & Aref, H. (1988). Chaotic advection in pulsed source–sink systems. *The Physics of Fluids*, *31*(3), 469–485. https://doi.org/10.1063/1.866828
Kapoor, V., & Kitanidis, P. K. (1998). Concentration fluctuations and dilution in aquifers. *Water Resources Research*, *34*(5), 1181–1193. https://doi.org/10.1029/97WR03608

Kitanidis, P. K. (1994). The concept of the dilution index. *Water Resources Research*, *30*(7), 2011–2026. https://doi.org/10.1029/94WR00762
Kitanidis, P. K., & McCarty, P. L. (2012). *Delivery and mixing in the subsurface: Processes and design principles for in situ remediation* (Vol. 4). Berlin, Germany: Springer Science & Business Media.
Kuo, C. H. (1972). Determination of reservoir properties from sinusoidal and multirate flow tests in one or more wells. *Society of Petroleum Engineers Journal*, *12*(6), 499–507. https://doi.org/10.2118/3632-PA
LaBolle, E. M., & Fogg, G. E. (2001). Role of molecular diffusion in contaminant migration and recovery in an alluvial aquifer system. *Transport in Porous Media*, *42*(1), 155–179. https://doi.org/10.1023/A:1006772716244
LeBlanc, D. R., Garabedian, S. P., Hess, K. M., Gelhar, L. W., Quadri, R. D., Stollenwerk, K. G., et al. (1991). Large-scale natural gradient tracer test in sand and gravel, Cape Cod, Massachusetts: 1. Experimental design and observed tracer movement. *Water Resources Research*, *27*(5), 895–910. https://doi.org/10.1029/91WR00241
Libera, A., de Barros, F. P. J., & Guadagnini, A. (2017). Influence of pumping operational schedule on solute concentrations at a well in randomly heterogeneous aquifers. *Journal of Hydrology*, *546*, 490–502. https://doi.org/10.1016/j.jhydrol.2016.12.022
Luo, J., Wu, W., Fienen, M. N., Jardine, P. M., Mehlhorn, T. L., Watson, D. B., et al. (2006). A nested-cell approach for in situ remediation. *Ground Water*, *44*(2), 266–274. https://doi.org/10.1111/j.1745-6584.2005.00106.x
Mackay, D. M., & Cherry, J. A. (1989). Groundwater contamination: Pump-and-treat remediation. *Environmental Science & Technology*, *23*(6), 630–636. https://doi.org/10.1021/es00064a001
Matheron, G., & De Marsily, G. (1980). Is transport in porous media always diffusive? A counterexample. *Water Resources Research*, *16*(5), 901–917. https://doi.org/10.1029/WR016i005p00901
Mays, D. C., & Neupauer, R. M. (2012). Plume spreading in groundwater by stretching and folding. *Water Resources Research*, *48*, W07501. https://doi.org/10.1029/2011WR011567
Metcalfe, G., Lester, D., Ord, A., Kulkarni, P., Rudman, M., Trefry, M., et al. (2010). An experimental and theoretical study of the mixing characteristics of a periodically reoriented irrotational flow. *Philosophical Transactions of the Royal Society of London A: Mathematical, Physical and Engineering Sciences*, *368*(1918), 2147–2162. https://doi.org/10.1098/rsta.2010.0037
Mulligan, C. N., Yong, R. N., & Gibbs, B. (2001). Remediation technologies for metal-contaminated soils and groundwater: An evaluation. *Engineering Geology*, *60*(1–4), 193–207. https://doi.org/10.1016/S0013-7952(00)00101-0
Naff, R. L., Yeh, T.-C. J., & Kemblowski, M. W. (1988). A note on the recent natural gradient tracer test at the Borden site. *Water Resources Research*, *24*(12), 2099–2103. https://doi.org/10.1029/WR024i012p02099
National Research Council. (1994). *Alternatives for ground water cleanup*. Washington, DC: National Academies Press. https://doi.org/10.17226/2311
Neuman, S. P., Winter, C. L., & Newman, C. M. (1987). Stochastic theory of field-scale fickian dispersion in anisotropic porous media. *Water Resources Research*, *23*(3), 453–466. https://doi.org/10.1029/WR023i003p00453
Neupauer, R. M., Meiss, J. D., & Mays, D. C. (2014). Chaotic advection and reaction during engineered injection and extraction in heterogeneous porous media. *Water Resources Research*, *50*, 1433–1447. https://doi.org/10.1002/2013WR014057
Ottino, J. M. (1989). *The kinematics of mixing: Stretching, chaos, and transport* (Vol. 3). Cambridge, UK: Cambridge University Press.
Paul, E. L., Atiemo-Obeng, V. A., & Kresta, S. M. (2004). *Handbook of industrial mixing: Science and practice*. Hoboken, NJ: John Wiley.
Piscopo, A. N., Kasprzyk, J. R., & Neupauer, R. M. (2015). An iterative approach to multi-objective engineering design: Optimization of engineered injection and extraction for enhanced groundwater remediation. *Environmental Modelling & Software*, *69*, 253–261. https://doi.org/10.1016/j.envsoft.2014.08.030
Piscopo, A. N., Neupauer, R. M., & Kasprzyk, J. R. (2016). Optimal design of active spreading systems to remediate sorbing groundwater contaminants in situ. *Journal of Contaminant Hydrology*, *190*, 29–43. https://doi.org/10.1016/j.jconhyd.2016.03.005
Piscopo, A. N., Neupauer, R. M., & Mays, D. C. (2013). Engineered injection and extraction to enhance reaction for improved in situ remediation. *Water Resources Research*, *49*, 3618–3625. https://doi.org/10.1002/wrcr.20209
Rabinovich, A., Barrash, W., Cardiff, M., Hochstetler, D. L., Bakhos, T., Dagan, G., et al. (2015). Frequency dependent hydraulic properties estimated from oscillatory pumping tests in an unconfined aquifer. *Journal of Hydrology*, *531*, 2–16. https://doi.org/10.1016/j.jhydrol.2015.08.021
Rehfeldt, K. R., & Gelhar, L. W. (1992). Stochastic analysis of dispersion in unsteady flow in heterogeneous aquifers. *Water Resources Research*, *28*(8), 2085–2099. https://doi.org/10.1029/92WR00750
Renner, J., & Messar, M. (2006). Periodic pumping tests. *Geophysical Journal International*, *167*(1), 479. https://doi.org/10.1111/j.1365-246X.2006.02984.x
Rodríguez-Escales, P., Fernández-Garcia, D., Drechsel, J., Folch, A., & Sanchez-Vila, X. (2017). Improving degradation of emerging organic compounds by applying chaotic advection in managed aquifer recharge in randomly heterogeneous porous media. *Water Resources Research*, *53*, 4376–4392. https://doi.org/10.1002/2016WR020333
Rubin, Y. (2003). *Applied stochastic hydrogeology*. Oxford, UK: Oxford University Press.
Sposito, G. (2006). Chaotic solute advection by unsteady groundwater flow. *Water Resources Research*, *42*, W06D03. https://doi.org/10.1029/2005WR004518
Suthersan, S., Killenbeck, E., Potter, S., Divine, C., & LeFrancois, M. (2015). Resurgence of pump and treat solutions: Directed groundwater recirculation. *Groundwater Monitoring & Remediation*, *35*(2), 23–29. https://doi.org/10.1111/gwmr.12114
Trefry, M. G., Lester, D. R., Metcalfe, G., Ord, A., & Regenauer-Lieb, K. (2012). Toward enhanced subsurface intervention methods using chaotic advection. *Journal of Contaminant Hydrology*, *127*(1), 15–29.
Weeks, S. W., & Sposito, G. (1998). Mixing and stretching efficiency in steady and unsteady groundwater flows. *Water Resources Research*, *34*(12), 3315–3322. https://doi.org/10.1029/98WR02535
Zarlenga, A., de Barros, F. P. J., & Fiori, A. (2016). Uncertainty quantification of adverse human health effects from continuously released contaminant sources in groundwater systems. *Journal of Hydrology*, *541*, Part B, 850–861. https://doi.org/10.1016/j.jhydrol.2016.07.044
Zhang, P., DeVries, S. L., Dathe, A., & Bagtzoglou, A. C. (2009). Enhanced mixing and plume containment in porous media under time-dependent oscillatory flow. *Environmental Science & Technology*, *43*(16), 6283–6288. https://doi.org/10.1021/es900854r
Zhang, Z., & Brusseau, M. L. (1999). Nonideal transport of reactive solutes in heterogeneous porous media: 5. Simulating regional-scale behavior of a trichloroethene plume during pump-and-treat remediation. *Water Resources Research*, *35*(10), 2921–2935. https://doi.org/10.1029/1999WR900162